Ruling out a saddle-point mechanism of ionization in intermediate-energy ion-atom collisions

K. H. Spicer,[1,*] C. T. Plowman,[1] N. W. Antonio,[1] M. S. Schöffler,[2] M. Schulz,[3] and A. S. Kadyrov[1,4]

[1]*Department of Physics and Astronomy, Curtin University, GPO Box U1987, Perth, Western Australia 6845, Australia*

[2]*Institut für Kernphysik, Universität Frankfurt, 60438 Frankfurt, Germany*

[3]*Physics Department and LAMOR, Missouri University of Science & Technology, Rolla, Missouri 65409, USA*

[4]*Institute of Nuclear Physics, Ulugbek, Tashkent 100214, Uzbekistan*

(Received 3 April 2024; accepted 17 May 2024; published 10 June 2024)

Is there a saddle-point mechanism for ionization in intermediate-energy ion-atom collisions? Since Olson [Phys. Rev. A **33**, 4397 (1986)] proposed the idea that the electrons stranded in the potential saddle between the two Coulomb centers dominate the ejected-electron spectra, multiple experimental and theoretical attempts have been made to answer this question. However, the topic has remained controversial. Here we provide a theoretical analysis of this question which can contribute significantly to a definitive answer, at least for intermediate and large projectile energies. To this end we calculate the energy and angular distribution of electrons emitted in proton-helium collisions. We use the two-center four-body wave-packet convergent close-coupling method based on the correlated two-electron structure for the helium target. The doubly differential cross sections obtained at 52 and 103 keV show no sign of a hump near one-half the relative velocity of the collision, which is expected according to the saddle-point ionization theory. At the same time, the results are in excellent agreement with measurements by Meckbach *et al.* [J. Phys. B **24**, 3763 (1991)]. Two mechanisms for the production of electrons are clearly identified: direct ionization (direct knockout) and electron capture to the continuum (ECC) of the projectile. The electron speed (equivalently, energy) where direct ionization peaks is found to be practically independent of the ejection angle. However, the ECC peak is shown to shift towards one-half the relative velocity with increasing electron angle. It is concluded that the signatures of the suggested saddle-point mechanism may actually be due to a shift of the well-known ECC peak when electrons are emitted into angles away from the forward direction. Thus, the answer to the question is in the negative.

DOI: 10.1103/PhysRevA.109.062805

I. INTRODUCTION

Ionizing collisions between ions and atoms represent one of the most fundamental physical processes and hence continue to be an area of active research [1–4]. Obtaining the most detailed information describing ionization, the differential cross sections, represents a considerable challenge both experimentally and theoretically. Recent advances in experimental techniques, such as cold target recoil ion momentum spectroscopy (COLTRIMS), have enabled measurements of the fully differential cross section (FDCS) in kinematically complete experiments [5]. However, calculating the doubly and fully differential cross sections requires highly accurate theoretical models which are very complex and computationally demanding, especially in the low- and intermediate-energy region where two-center effects must be accounted for. Despite these challenges, continued interest in differential ionization arises from a lack of clarity regarding the specific mechanisms governing ionization [6].

In intermediate-energy ion-atom collisions, there are two widely recognized mechanisms for single ionization: direct ionization (DI) and electron capture to the continuum (ECC). The former represents direct knockout of the target electron by the projectile and is characterized by a maximum when the electron is ejected with near-zero energy. The latter is characterized by a strong peak, most prominent in the forward direction when the electron velocity $\boldsymbol{v}_e$ matches the projectile velocity $\boldsymbol{v}_P$ relative to the target. Early studies [7,8] employing modified first-order perturbative methods predicted that the ECC peak would have a nearly symmetric form. However, this was not reflected in experimental data, which notably skewed toward lower electron velocities [9,10], though the reason for the discrepancy was not yet understood. In their study of 170 keV proton collisions with helium, Meckbach *et al.* [11] observed the expected peaks near the target and the projectile in the velocity distributions of forward-ejected electrons. They also noted the skew in the ECC peak which formed a wide ridge connecting with the DI peak. The origin of this ridge was not attributed to either of the two established ionization mechanisms. Instead, analogies were made to a Wannier-type mechanism typically understood within electron-atom scattering as the ionization phenomenon of electrons moving in opposite directions with the target ion remaining midway between the two [12]. This was later extended theoretically to positron scattering on atoms by Klar [13]. Olson [14] proposed that in the case of a heavy projectile, the ejected electron would be stranded at the point between the scattered projectile and residual target at which the Coulombic attraction from the two is equal. In the charge-symmetric case this is expected

*Contact author: kate.bain@postgrad.curtin.edu.au

to occur when the electron is ejected with half the projectile speed $v_P/2$. If instead the system was charge asymmetric, the location of the corresponding point is determined by $v_P/[1 + (Z_P/Z_T)^{1/2}]$ [15], where the effective nuclear charges of the projectile and target are Z_P and Z_T, respectively. According to this idea, as the residual target ion and projectile move apart, the active electron gets stranded between them, leading to an increase in the ionization probability in this region. Olson [14] claimed that the electrons stranded between the two Coulomb centers dominate the ejected-electron spectra. This ion-atom counterpart to the Wannier mechanism was termed saddle-point ionization [16].

This idea was supported by classical-trajectory Monte Carlo (CTMC) [14,17] and triple-center coupled-channel [18] calculations of the total and singly differential cross sections for the proton-hydrogen system. Presenting both an experimental and CTMC study of 60–200 keV proton ionization of helium, Olson *et al.* [16] claimed to have found further evidence for the existence of saddle-point ionization. The CTMC results for the doubly differential cross section (DDCS) for ionization as a function of the speed of the electron at an emission angle of 17° peaked around the so-called saddle point. The experimental measurements exhibited a peak between $v_e/v_P = 0$ and 1; however, the exact positions of the peaks were somewhat misaligned with the CTMC data. Ultimately, Olson *et al.* [16] concluded that there was general agreement between the sets of data and that both the CTMC and experiment showed that saddle-point electrons dominate ionizing collisions in the intermediate-energy range. As the location of the peak is significant for proving, or alternatively disproving, saddle-point ionization theory, this discrepancy brings these conclusions into question.

Subsequent investigations by Irby *et al.* [19] and Gay *et al.* [15] of both proton and He^{2+} collisions with helium in the intermediate-energy region drew the same conclusion. In particular, they noted an inward shift of the peak position in the charge-asymmetric He^{2+} experiment. Interestingly, the corresponding CTMC calculations [19] did not predict such a shift.

Meanwhile, Bernardi *et al.* [20] revisited the results of Meckbach *et al.* [11] and determined that the original experiment was affected by instrumental error. The conclusions made regarding the saddle-point peak were retracted. This was followed by a number of publications [21–23] aimed at questioning the existence of saddle-point electrons. The focal point of their argument was that the mode of presentation of the DDCS can affect the conclusions drawn. It should be noted, however, that true physical phenomena should be independent of presentation. In these works, the *p*-He and He^{2+}-He systems were studied. The DI and ECC peaks were identified in the electron velocity distribution. The ridge connecting the two peaks was reproduced by the two-center continuum-distorted-wave eikonal-initial-state (CDW-EIS) approach which accounted for the asymmetry of the ECC peak. In the forward direction, the ECC peak was most prominent and began to shift monotonically toward smaller electron speeds as the ejection angle increased. The recent measurements of the FDCS by Dhital *et al.* [24] support this trend. Furthermore, the position of the maximum was not found to depend on the charge of the projectile. These findings were later corroborated by DuBois [25], who experimentally investigated the same collision systems. The results were found to be in agreement with the works of Bernardi *et al.* It was suggested that the measurements of Irby *et al.* [19] and Gay *et al.* [15], particularly those for He^{2+} impact, were in error. However, the saddle-point controversy persisted. In part, this was because no high-order theory was available which was capable of confirming the picture of ionization presented by Bernardi *et al.* [21–23] and DuBois [25].

In further contradiction to the claims of Bernardi *et al.* and DuBois, a variety of methods were applied to model proton-hydrogen and proton-helium collisions in the intermediate-energy range, all of which in fact supported the existence of the saddle-point mechanism. For proton-impact ionization of hydrogen, a lattice method was employed by Gavras *et al.* [26], and the two-center momentum-space discretization approach was used by Sidky and Lin [27]. Both presented time sequence electron density plots and concluded that the saddle-point mechanism existed. In the proton-helium case, the CTMC and CDW-EIS methods applied by Kravis *et al.* [28], as well as two further experiments [28,29], also found saddle-point electrons and identified three separate mechanisms: DI, saddle-point ionization, and ECC. Other systems, such as C^{q+}-He, were also investigated at intermediate energies in an attempt to clarify the issue of saddle-point ionization. Irby *et al.* [30] observed the projectile-charge-dependent shifts expected for saddle-point emission; however, DuBois [31] performed the same measurements which, once again, failed to support the conclusions of Irby *et al.* [30]. Nonetheless, without supporting theoretical evidence, this did not resolve the issue and the subject remains a topic of debate [32].

Sidky *et al.* [33] calculated three-dimensional ejected-electron momentum distributions for proton impact ionization of atomic hydrogen for impact energies of 10–50 keV. The distributions showed a peak in the longitudinal momentum at half the projectile impact velocity. However, based on quantum and classical analyses, these authors concluded that this peak is a false indicator for the saddle-point mechanism. Furthermore, they showed that the influence of the potential saddle on ionization decreases rapidly from 10 to 50 keV. It must be noted, however, that the distributions presented in Ref. [33] isolate small parts of the space. Nevertheless, this was the first theoretical work that questioned the validity of the saddle-point ionization mechanism in the intermediate-energy region. Presenting results at 30, 40, 60, and 100 keV, Nesbitt *et al.* [34] investigated the DDCS for forward ionization using the CDW-EIS approach. The ECC peak was identified as the dominant feature, showing little evidence for saddle-point ionization except at 100 keV where a broad ridge is observed and attributed to this mechanism. Notably, these results did not display the electron-ejection angle-dependent shift previously identified by Bernardi *et al.* [21–23]. Later, using COLTRIMS, Schmidt *et al.* [35] investigated the production of free electrons in slow He^{2+}-He collisions in the energy region 9–28 keV/u. These authors measured the electron velocity distribution in various planes state selective with respect to the second electron that remained bound. They revealed that, in contrast to the classical saddle-point ionization model, most of the reaction channels display a local minimum of the electron velocity distribution at exactly the saddle point

of the potential of the two Coulomb centers. However, these works were also unable to change the perception on saddle-point ionization. Very recently, Schmidt *et al.* [36] reported experimental measurements of the velocity distributions of electrons emitted in ionization of He by 10–45 keV proton impact. While the low-energy results were interpreted in terms of the saddle-point ionization, the intermediate-energy results showed that an accumulation of the electron velocity distribution at the nuclei becomes more pronounced. In particular, the results at 45 keV proton impact do not show any concentration of electrons with speed about $v_P/[1 + (Z_P/Z_T)^{1/2}]$ that could be associated with the saddle-point mechanism.

While this controversy persisted for intermediate-energy collisions, Pieksma *et al.* [37] found strong experimental and theoretical evidence for the existence of a saddle-point ionization mechanism in p-H collisions at energies of 1–6 keV. Bandarage and Parson [38] applied the CTMC approach to 4–25 keV total ionization cross sections for proton-hydrogen collisions and found that saddle-point ionization makes a large contribution, decreasing with increasing projectile velocity. Total ionization cross sections were calculated with the hidden-crossings theory for both the p-H and He^{2+}-H systems [39], where the inclusion of the saddle-point mechanism improved the agreement of the cross section with experimental measurements. The p-H, He^{2+}-H, and p-He systems were investigated further at 1, 2, 4, and 6 keV/u through differential momentum distributions [37,40]. Overall, it was found that the cross sections displayed a peak at the saddle point for collision energies of 4 and 6 keV/u, which was shifted in the He^{2+}-H case. Somewhat unexpectedly, at 1 and 2 keV/u, results did not support saddle-point ionization. It was argued that at these low energies, molecular effects are dominant. Dörner *et al.* [41] presented two-dimensional velocity distributions of electrons emitted in p-He collisions at 5–15 keV. Both the experimental data and CTMC results showed nearly all of the electrons being ejected in a broad range centered around the saddle point. Illescas *et al.* [42] concurred with their study of He^{2+} collisions on hydrogen. Schultz *et al.* [43] directly solved the time-dependent Schrödinger equation on a numerical lattice to investigate the problem for the p-H system. Overall, these classical and semiclassical studies determined that while there is evidence for a saddle-point mechanism for low projectile velocities, the picture was less clear at higher velocities. In the present paper we do not consider the low-energy region; instead we focus on the energy region above 25 keV.

Despite the lack of sufficient evidence to either support or negate the existence of a saddle-point ionization mechanism at intermediate energies, the concept was generally accepted and continues to be made reference to. Existing theories capable of calculating differential cross sections in the kinematic regimes where saddle-point ionization is predicted to occur were either low-order perturbative approaches or limited to a certain part of the space, for instance, calculations at a fixed value of the impact parameter or internuclear distance. However, it is known that a wide range of impact parameters and internuclear distances contribute to the final outcome and therefore substantive conclusions about overarching ionizations mechanisms for the entire space could not be made based on these results. For these reasons, the conclusions drawn from these findings were unable to settle the debate. The more sophisticated configuration-space lattice method [26] and two-center momentum-space discretization method [27] for solving the time-dependent Schrödinger equation supported the saddle-point ionization mechanism. Attempts to extend the adiabatic hidden-crossing theory (which is valid, strictly speaking, only if $v_P \ll v_0$, where v_0 is the classical speed of the electron in the Bohr orbit) to intermediate-energy region did not lead to any practical results for differential ionization observable in the experiment (see Ref. [32] and references therein). High-order close-coupling methods have yet to be applied to this problem as the conventional implementations have not been able to calculate the amplitudes required for differential ionization. The wave-packet convergent close-coupling (WP-CCC) approach [44] has been developed to determine these amplitudes. It has previously been used to model differential ionization in proton-atomic hydrogen [45,46] and proton-helium [47–49] collisions. The approach has also been applied to differential ionization in p-H_2 [50–52] and He^{2+}-He [53,54] collisions. The results on the integrated, singly and doubly differential cross sections were consistently in very good agreement with available experimental data.

In this work the WP-CCC method is applied to the calculation of the energy and angular distribution of electrons emitted in 52 and 103 keV proton collisions with helium. The obtained doubly differential cross sections for single ionization are presented in three forms: the cross sections differential in electron speed and angle, electron velocity, and electron energy and angle. The aim of this paper is to provide a clear answer to the question about whether or not there is a saddle-point ionization mechanism in intermediate-energy collisions between protons and helium atoms.

Unless specified otherwise, atomic units are used throughout this paper.

II. TWO-CENTER WAVE-PACKET CONVERGENT CLOSE-COUPLING METHOD

The WP-CCC approach employs the semiclassical approximation in the impact-parameter representation. Various aspects of the approach have been described in Refs. [44,45]. The extension of the method to the four-body p-He problem based on the correlated two-electron wave function for the helium target has been detailed in Ref. [55]. Here a brief description specific to doubly differential ionization is given. Beginning with the exact nonrelativistic time-independent Schrödinger equation, we substitute the four-body total scattering wave function which develops from the initial channel representing a proton incident on ground-state helium. The bases representing the target and projectile consist of eigenstates for the bound spectrum and wave-packet pseudostates for the continuum. The wave packets are formed by discretizing the continuum, up to some sufficiently large energy, into bins and integrating the true continuum wave function over the corresponding bin in momentum space. Then applying the frozen-core approximation where one electron is kept in the $1s$ state throughout the collision, along with the semiclassical approximation, we obtain a set of coupled first-order differential equations which is solved numerically using the Runge-Kutta method for the time-dependent expansion coefficients. These

coefficients are then used to determine transition amplitudes for ionization. For further details, see Refs. [44,45].

There are three types of DDCS [48]. The DDCS relevant to the present work is the one differential in the energy and angle of the ejected electron. It can also be represented in momentum space. In our case, the latter is equivalent to velocity space. The DDCS differential in the energy and angle of the ejected electron is obtained by numerically integrating the fully differential cross section $d^3\sigma/dE_e d\Omega_e d\Omega_f$ over the solid angle of the projectile Ω_f in the final channel f as

$$\frac{d^2\sigma}{dE_e d\Omega_e} = \int \frac{d^3\sigma}{dE_e d\Omega_e d\Omega_f} d\Omega_f, \tag{1}$$

where Ω_e is the solid angle that the electron is ejected into and $E_e = v_e^2/2$ is the ejected-electron energy. The FDCS itself is given as the combination of the DI and ECC components [48]. For further discussion $d^2\sigma/dE_e d\Omega_e$ is denoted by DDCS(E_e, Ω_e). It can be transformed into velocity space to give the cross section differential in the speed and angle of the ejected electron, denoted by DDCS(v_e, Ω_e), as

$$\frac{d^2\sigma}{dv_e d\Omega_e} = v_e \frac{d^2\sigma}{dE_e d\Omega_e}, \tag{2}$$

where v_e is the speed of the ejected electron. Furthermore, the cross section differential in the velocity of the electron $\boldsymbol{v}_e$, denoted DDCS($\boldsymbol{v}_e$), is given by[1]

$$\frac{d^2\sigma}{d\boldsymbol{v}_e} = \frac{1}{v_e} \frac{d^2\sigma}{dE_e d\Omega_e}. \tag{3}$$

As these three cross sections represent the same physical process, the same conclusions about physical processes should be drawn from all of them.

In the practical calculations, the number of negative- and positive-energy pseudostates included in the calculations was increased until satisfactory convergence was achieved. The parameters of the basis used in the calculations were quite similar to those used in our previous calculations for this collision system [47,48]. Specifically, at 52 keV, a basis containing bound states up to principal quantum number 10 and 25 bin states discretizing the continuum for each orbital angular momentum $\ell \leqslant 6$ was used on both centers. At 103 keV, the number of bins was increased to 30; however, the maximum required ℓ to reach convergence was 5. In both cases, the continuum was discretized up to a maximum ejected-electron momentum of $\kappa_{max} = 5$ a.u., which was found to be sufficient for the results to converge. The position of the projectile was incremented along the z axis from $z_{min} = -200$ a.u. to $z_{max} = 200$ a.u. for all impact parameters. There were 600 z points distributed exponentially, with the density being greatest at the collision center. Impact parameters ranged from 0 to 20 a.u., which was sufficient to allow for the probability of all collision processes to fall off several orders of magnitude.

[1]In this work we follow the traditional notation and label the quantities given in Eqs. (1)–(3) as DDCS. Strictly speaking, they are triply differential cross sections and the FDCS is a fivefold differential cross section.

III. RESULTS

As described above, the DDCS for ionization can be represented in three equivalent formats. They are calculated using Eqs. (1)–(3). These cross sections are given in the laboratory frame in energy space, and velocity space. The results obtained at incident projectile velocities of 52 and 103 keV are presented below as functions of v_e/v_P. Calculations were performed for the entire range of electron-ejection angles from the forward direction to the backward one. However, the results are presented up to an electron-ejection angle of 45°, the region where the probability of ionization is highest.

Figure 1 presents the DDCS for electrons ejected at angles of 0°, 2°, 7°, 10°, and 20° obtained with the WP-CCC approach for a projectile energy of 52 keV in comparison with the experimental data by Meckbach *et al.* [23]. The experimental data, originally given in arbitrary units, are normalized to the present absolute values. The data for 0°, 10°, and 20° were retrieved from Fig. 2 and the data for 2° and 7° from Fig. 3 of the relevant paper. It is noteworthy that there was a factor of 0.65 difference between these two sets of experimental data. It should also be noted that in the region of the cusp, the measured cross sections become extremely sensitive to the experimental resolution and may contribute to discrepancies.

The left column in Fig. 1 shows the cross section differential in the speed and angle of the ejected electron, the middle column is differential in the ejected-electron energy and angle, and the right column is differential in the velocity of the ejected electron. The experimental data for DDCS(E_e, Ω_e) are deduced from the DDCS(v_e, Ω_e) measurements by Meckbach *et al.* [23]. In all panels, the present WP-CCC results are given by solid lines connecting the points corresponding to the energies of the wave-packet pseudostates.

Overall, we find very good agreement with the measurements of Meckbach *et al.* [23] at all ejection angles shown. Agreement is good for all three representations of the DDCS. This is not surprising as the underlying physics is the same and hence the agreement (or disagreement) in one should be reflected in the other two. In other words, for the purpose of comparing with experiment, the choice of the format is immaterial and the results shown in Fig. 1 clearly demonstrate this. Furthermore, if we aim to extract information about underlying physics from the results, our conclusions should be independent of the choice of representation for the cross section. We can see, however, that depending on the format in which the DDCS is presented, certain parts of the space may be enhanced or, alternatively, suppressed. Taking the DDCS(E_e, Ω_e) as a reference point, we see that the DDCS($\boldsymbol{v}_e$) enhances the kinematic region where slow electrons are emitted, while the same region is suppressed in the DDCS(v_e, Ω_e). We emphasize that the ionization amplitude that gives all three of these DDCS is the same. In other words, the aforementioned enhancement or suppression are artifacts of the presentation format and just reflect whether the DDCS(E_e, Ω_e) is divided or multiplied by v_e [see Eqs. (2) and (3)]. Another important conclusion we can draw from Fig. 1 is that the DDCS($\boldsymbol{v}_e$) is not a very convenient format for presenting physical results as it blows up in the part of the kinematic region corresponding to the emission of low-energy electrons, obscuring the rest of the collision space.

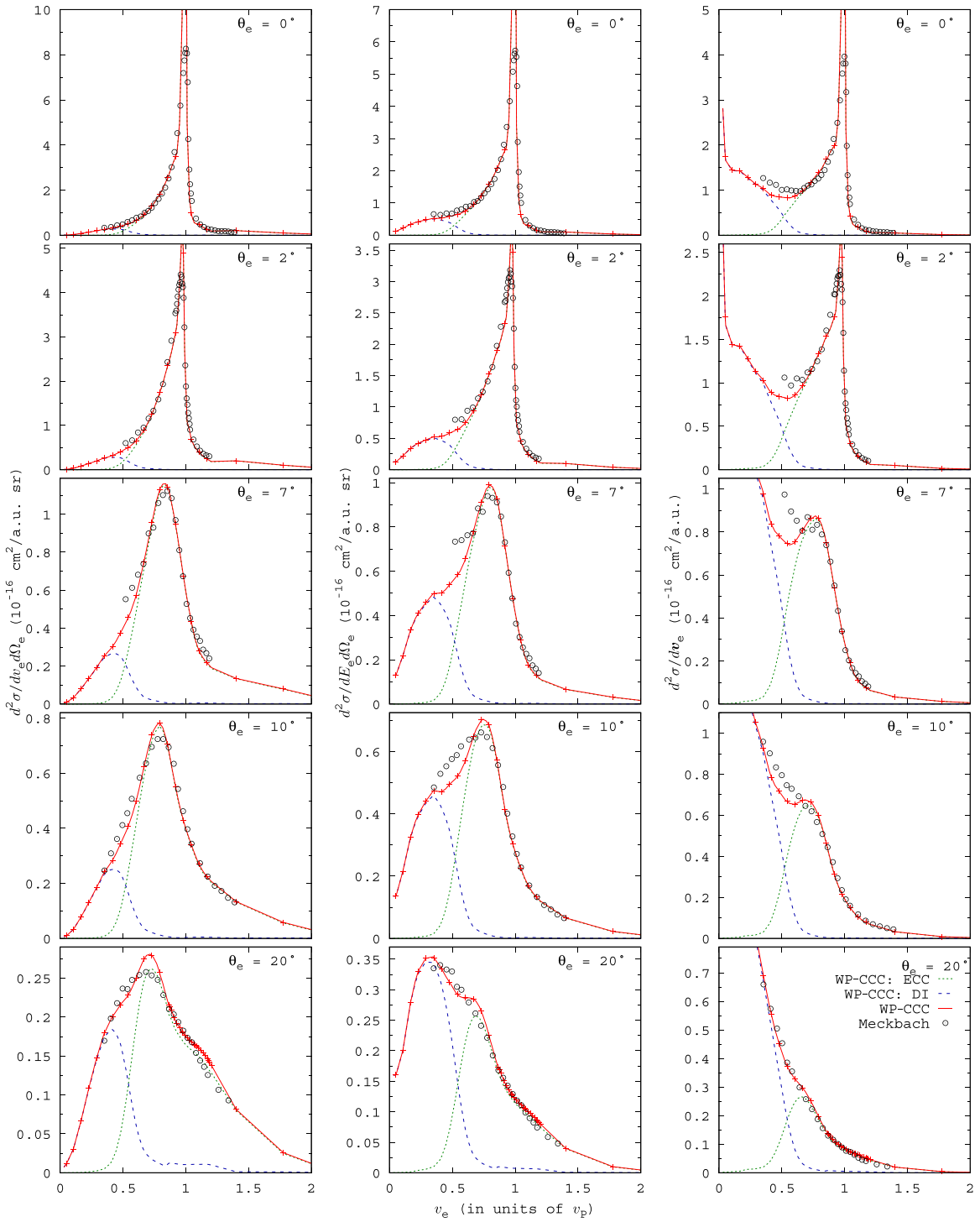

FIG. 1. Doubly differential cross section for p-He ionization at 52 keV. The WP-CCC results are compared with data from Meckbach *et al.* [23]. The DI and ECC components are also shown. The key in the bottom right panel applies to all panels.

In the past, selecting a particular mode of presentation was a point of contention for interpreting data. Meckbach *et al.* [23] proposed that the DDCS($\boldsymbol{v}_e$) is the optimal form for presenting results as it remains unaltered when transforming between the target and projectile frames. Other authors [15] preferred the form of DDCS(v_e, Ω_e) due to its accentuation of the region between the target and projectile. Olson *et al.* [16] presented the DDCS(v_e, Ω_e) at an ejection angle of 17° as proof of the saddle-point ionization mechanism. This seemingly contradicts saddle-point theory, which asserts that the strongest saddle-point peak in the DDCS(v_e, Ω_e) is expected in the forward direction. According to the experimental measurements [23] and the present WP-CCC calculations, this is not the case. As seen in all three columns of Fig. 1, the results for 0° and 2° are dominated by a sharp peak when the electron velocity matches or closely matches the projectile velocity,

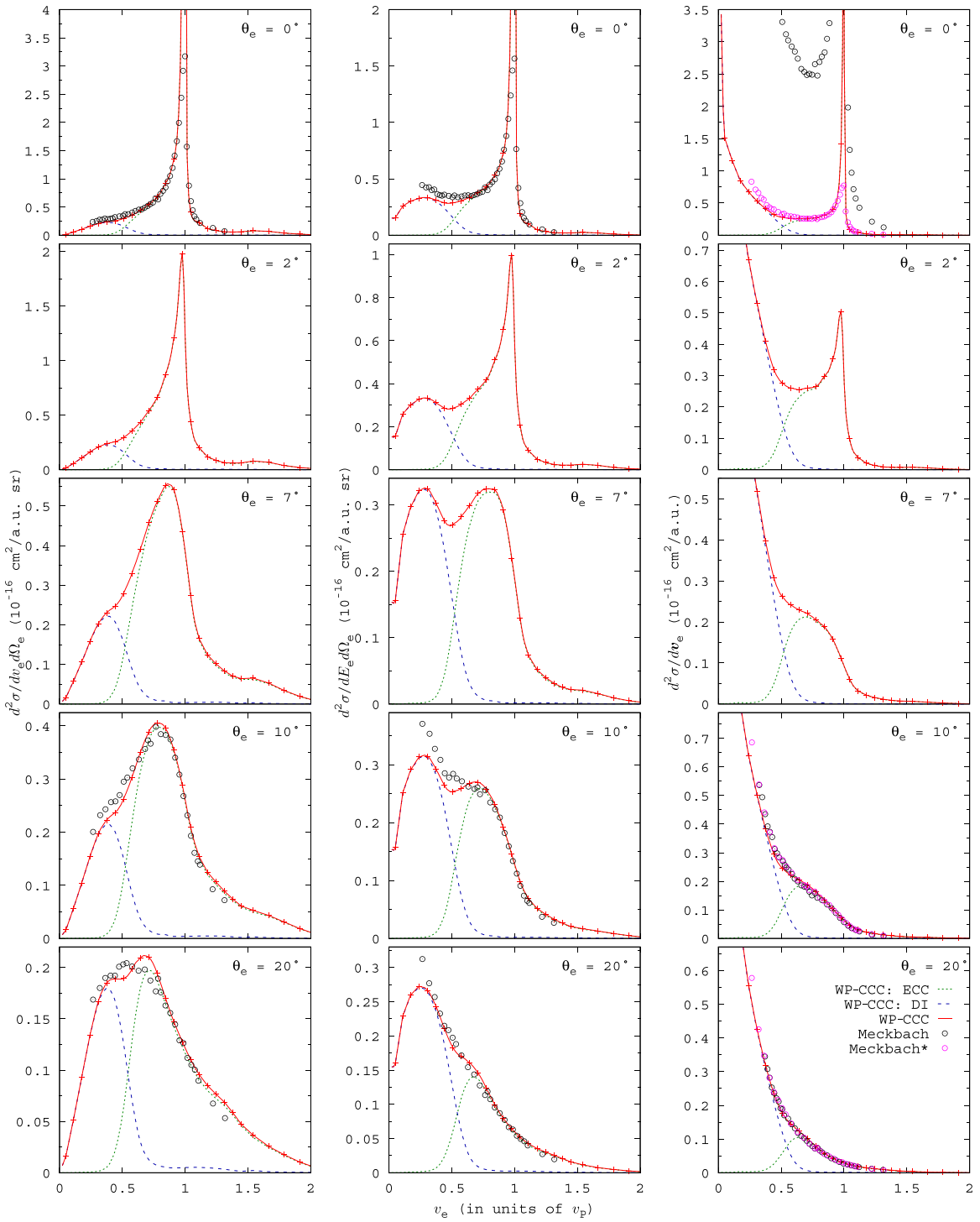

FIG. 2. Same as in Fig. 1 but for 103 keV protons.

respectively. It is commonly recognized as the ECC peak. There is no evidence of a saddle-point peak around $v_e = v_P/2$ in any of the three formats.

The rationale provided by Olson *et al.* [16] for displaying larger angles was that, in the narrow forward direction, the ECC mechanism dominates the cross section while its contribution quickly diminishes away from 0°. To address this assertion, we calculated the DI and ECC components of the DDCS separately. In Fig. 1 these are shown by the long-dashed and short-dashed lines, respectively. We can clearly see that the maximum of the DDCS(v_e, Ω_e) for all angles shown is purely due to the ECC component of the cross section. It is interesting to note that its peak position in v_e/v_P moves toward 0.5 with increasing angle. At the same time, as the emission angle increases, the relative contribution of DI grows. In the DDCS(E_e, Ω_e), the magnitudes of the ECC and DI peaks become comparable around 15° (not shown). At 20°, the DI peak is larger than the ECC one. This moves

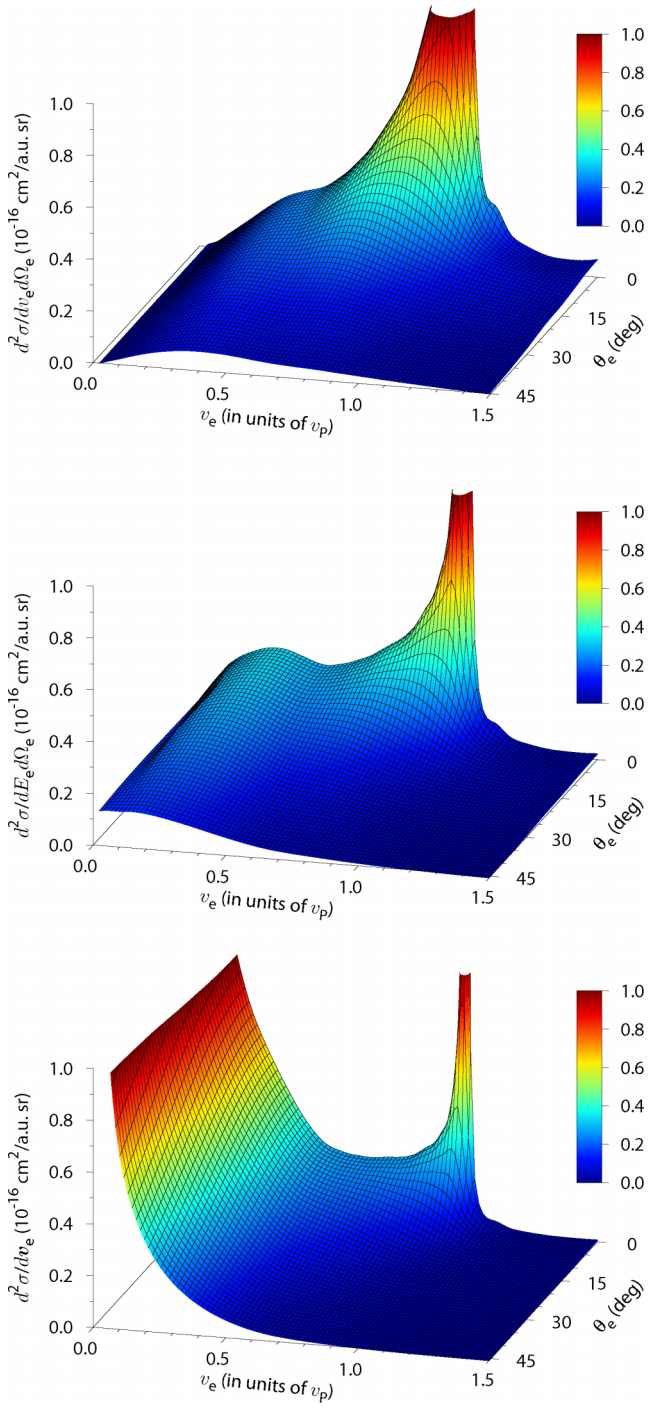

FIG. 3. Doubly differential cross section for p-He ionization at 103 keV as a function of electron ejection energy and angle. The WP-CCC results are given.

the peak of the DDCS(E_e, Ω_e) across the $v_e/v_P = 0.5$ point. On the other hand, since the DI peak is suppressed in the DDCS(v_e, Ω_e), this cross section still peaks on the other side of the $v_e/v_P = 0.5$ point. The same trend continues as the ejection angle increases. At sufficiently large angles, both the DDCS(v_e, Ω_e) and DDCS(E_e, Ω_e) peak where the DI component does while the ECC component become negligible. From Fig. 1 we see for both the experimental and WP-CCC DDCS that as the ejection angle increases, the peak of the DDCS(v_e, Ω_e) appears to shift towards $v_e/v_P = 0.5$. However, the peak position never reaches the $v_e/v_P = 0.5$ point even at large angles. In the case of the DDCS(E_e, Ω_e), it even appears to cross the $v_e/v_P = 0.5$ point when the angle reaches 20°. Thus, Figs. 1 and 2 illustrate the point that conclusions based solely on the presence of a peak somewhere between $v_e/v_P = 0$ and 1 should be heavily scrutinized. This further negates the claims of Olson *et al.* [16].

Thus, based on the WP-CCC results, which to a large extent agree with the experiment, one can conclude that the claim by Olson [14] about the electrons stranded between the two Coulomb centers at the saddle point dominating the ejected-electron spectra is not supported by the present results, at least at 52 keV.

Figure 2 presents the same cross sections as in Fig. 1 but for a projectile energy of 103 keV. As in Fig. 1 the agreement between the WP-CCC results and the experimental data by Meckbach *et al.* [23] is good where data are available. This figure reinforces the conclusions drawn above and extends them to higher energies. Thus, the conclusions are valid in the entire energy region where ionization is the dominant channel.

It must be noted that there may have been a minor error in the original presentation of the experimental data [23] for the DDCS($\boldsymbol{v}_e$) in the forward direction. The data labeled simply as "Meckbach" in the right column are taken directly from Fig. 1 of Ref. [23]. The data labeled as "Meckbach*" are the experimental points shown for the DDCS(v_e, Ω_e) transformed into the DDCS($\boldsymbol{v}_e$). The discrepancy between the two sets of data at 0° is a factor of 10. The data given in Ref. [23] for the other angles are consistent across the different formats.

Figure 3 presents the same three DDCSs as in Fig. 2 obtained using the WP-CCC method but in the form of a three-dimensional map for a wider range of electron-ejection angles, between 0° and 45° increasing in steps of 1°, and for electron speeds between 0 and $1.5v_P$. In all three types of DDCSs in this figure, we clearly see the monotonic shift of the ECC peak toward lower electron speeds with increasing ejection angle, confirming our conclusions over a wider angular range. At the same time, for all electron-ejection angles shown, the position of the DI peak does not show noticeable angular dependence.

IV. CONCLUSION

The prediction of Olson [14] that the electrons stranded between the two Coulomb centers should dominate the ejected-electron spectra has influenced research on ionization in intermediate-energy ion-atom collisions for almost four decades. The concept has been debated with some experiments supporting and some questioning it. Theory has lagged far behind, unable to provide a clear answer due to difficulties in calculating differential cross sections for ionization.

The four-body wave-packet convergent close-coupling approach has been applied to the calculation of cross sections differential in the electron speed and angle, electron velocity, and electron energy and angle for 52 and 103 keV proton collisions with helium. Results are found to be in excellent agreement with the experimental data by Meckbach *et al.* [23] and for all three modes of presentation. The present results show that changing the space in which the cross

sections are presented can emphasize, or alternatively suppress, certain kinematic regions. However, the conclusion drawn from all of them regarding the saddle point is consistent: There is no evidence to support saddle-point ionization as a separate mechanism at least at projectile energies above 50 keV. The DDCS(v_e, Ω_e), the cross section most commonly used to support the saddle-point theory, indeed displays a broad peak near $v_e = 0.5v_P$ at angles away from the forward direction. However, the results obtained in this work clearly demonstrate that this peak is produced by the gradual shift of the ECC peak from $v_e = v_P$ at 0° towards $v_e = 0.5v_P$ until the ECC mechanism is no longer relevant. This happens before the ECC peak reaches the $v_e = 0.5v_P$ point. As the ejection angle increases further, the DDCS(v_e, Ω_e) and DDCS(E_e, Ω_e) peak where the DI mechanism is dominant. This occurs at an electron velocity well under $0.5v_P$, the so-called saddle point. Therefore, nowhere in the electron spectrum do we observe a saddle-point ionization peak.

Thus, the WP-CCC method reveals a clear and understandable picture of differential ionization of helium by intermediate-energy proton impact. This is the most important region in terms of electron production as ionization is the dominant channel. No sign of the saddle-point mechanism of ionization has been seen. Furthermore, in the forward direction the results show a local minimum at the electron speed where, according to the saddle-point mechanism, a hump is expected, directly contradicting the prediction by Olson [14]. This makes sense from a physics point of view. In the Wannier case of two electrons in the field of a positively charged ion, the system reaches a stable equilibrium as the total energy goes to zero. However, when we have one electron in the field of two positively charged ions, the saddle point represents an unstable equilibrium as it is located at the maximum of the potential between the two heavy particles. Therefore, electrons at this point would be highly sensitive to even small perturbations. It is unlikely that they would get stranded at the potential hump to make ionization through this point significant, not to mention dominating the ejected-electron spectra. In addition to this, conclusions regarding ionization mechanisms made by Olson *et al.* [16] are based exclusively on the DDCS(v_e, Ω_e) representation. Equation (2) indicates that this cross section must approach zero as the electron-ejection speed approaches zero, thereby ensuring there will be a maximum somewhere between $v_e = 0$ and $v_e = v_P$ for any ejection angle. In Ref. [16], the maximum of the CTMC results occurs over a range of v_e/v_P between 0.3 and 0.6, varying with incident projectile energy. Therefore, the observation of a maximum does not seem to prove anything. Furthermore, the extrapolated CTMC results do not appear to approach zero at $v_e = 0$. This could be an artifact of the finite bin size in v_e and be indicative of limitations of the CTMC for calculating differential cross sections.

The present results do not exclude, however, that the saddle-point mechanism may play a role at sufficiently low energies. If that is the case, the boundary of this low-energy region, whether it is $v_P \ll v_0$ or just $v_P \lesssim v_0$, remains to be established.

An interesting direction for future work could be applying the WP-CCC approach to differential ionization in charge-asymmetric collision systems such as He^{2+} [15,19,25] and C^{q+} [28–31] scattering on helium, which still remain controversial. Another avenue is extension of the two-center WP-CCC approach to calculate the fully differential cross section for *p*-He ionization in the intermediate-energy region. At sufficiently high energies, where electron-capture channels can be neglected, the single-center WP-CCC method was applied to *p*-He ionization [56,57], leading to excellent agreement with the ultrahigh-resolution experiments [58,59]. Ionization in C^{6+}-He collisions at 100 MeV/amu was considered using a single-center quantum-mechanical implementation of the method [60]. However, this did not resolve the discrepancy between theory and experiment [61]. The features reported in [61] remain unexplained and a challenge for theory. The two-center WP-CCC may shed light on possible high-order effects that could not be seen with a single-center approach.

ACKNOWLEDGMENTS

This work was supported by the Australian Research Council. K.H.S. acknowledges support from the Forrest Research Foundation. K.H.S. and N.W.A. acknowledge support through an Australian Government Research Training Program Scholarship. M.S.S. acknowledges support from Deutsche Forschungsgemeinschaft and Bundesministerium für Bildung und Forschung. M.S. is grateful for support from the U.S. National Science Foundation under Grant No. PHY-2011307. The authors also acknowledge the resources and services of the Pawsey Supercomputer Centre and the National Computing Infrastructure.

[1] *Ion-Atom Collisions: The Few-Body Problem in Dynamic Systems*, edited by M. Schulz (De Gruyter, Berlin, 2019).

[2] *State-of-the-Art Reviews on Energetic Ion-Atom and Ion-Molecule Collisions*, edited by D. Belkić, I. Bray, and A. Kadyrov (World Scientific, Singapore, 2019).

[3] R. D. Rivarola, O. A. Fojón, M. Ciappina, and D. Crothers, in *Springer Handbook of Atomic, Molecular, and Optical Physics*, edited by G. W. F. Drake (Springer, Cham, 2023), pp. 813–828.

[4] T. Kirchner, A. L. Ford, and J. F. Reading, in *Springer Handbook of Atomic, Molecular, and Optical Physics* (Ref. [3]), pp. 785–794.

[5] M. Schulz, R. Moshammer, D. H. Madison, R. E. Olson, P. Marchalant, C. T. Whelan, H. R. J. Walters, S. Jones, M. Foster, H. Kollmus, A. Cassimi, and J. Ullrich, J. Phys. B **34**, L305 (2001).

[6] S. Bastola, M. Dhital, S. Majumdar, A. Hasan, R. Lomsadze, J. Davis, B. Lamichhane, S. Borbély, L. Nagy, and M. Schulz, Atoms **10**, 119 (2022).

[7] J. Macek, Phys. Rev. A **1**, 235 (1970).

[8] A. Salin, J. Phys. B **5**, 979 (1972).

[9] M. Rodbro and F. D. Andersen, J. Phys. B **12**, 2883 (1979).

[10] W. Meckbach, I. B. Nemirovsky, and C. R. Garibotti, Phys. Rev. A **24**, 1793 (1981).
[11] W. Meckbach, P. J. Focke, A. R. Goñi, S. Suárez, J. Macek, and M. G. Menendez, Phys. Rev. Lett. **57**, 1587 (1986).
[12] G. H. Wannier, Phys. Rev. **90**, 817 (1953).
[13] H. Klar, J. Phys. B **14**, 4165 (1981).
[14] R. E. Olson, Phys. Rev. A **33**, 4397 (1986).
[15] T. J. Gay, M. W. Gealy, and M. E. Rudd, J. Phys. B **23**, L823 (1990).
[16] R. E. Olson, T. J. Gay, H. G. Berry, E. B. Hale, and V. D. Irby, Phys. Rev. Lett. **59**, 36 (1987).
[17] R. E. Olson, Phys. Rev. A **27**, 1871 (1983).
[18] T. G. Winter and C. D. Lin, Phys. Rev. A **29**, 3071 (1984).
[19] V. D. Irby, T. J. Gay, J. W. Edwards, E. B. Hale, M. L. McKenzie, and R. E. Olson, Phys. Rev. A **37**, 3612 (1988).
[20] G. Bernardi, S. Suárez, P. Focke, and W. Meckbach, Nucl. Instrum. Methods Phys. Res. Sect. B **33**, 321 (1988).
[21] G. C. Bernardi, S. Suárez, P. D. Fainstein, C. R. Garibotti, W. Meckbach, and P. Focke, Phys. Rev. A **40**, 6863 (1989).
[22] G. Bernardi, P. Fainstein, C. R. Garibotti, and S. Suarez, J. Phys. B **23**, L139 (1990).
[23] W. Meckbach, S. Suarez, P. Focke, and G. Bernardi, J. Phys. B **24**, 3763 (1991).
[24] M. Dhital, S. Bastola, A. Silvus, J. Davis, B. R. Lamichhane, E. Ali, M. F. Ciappina, R. Lomsadze, A. Hasan, D. H. Madison, and M. Schulz, Phys. Rev. A **102**, 032818 (2020).
[25] R. D. DuBois, Phys. Rev. A **48**, 1123 (1993).
[26] P. Gavras, M. S. Pindzola, D. R. Schultz, and J. C. Wells, Phys. Rev. A **52**, 3868 (1995).
[27] E. Y. Sidky and C. D. Lin, Phys. Rev. A **60**, 377 (1999).
[28] S. D. Kravis, M. Abdallah, C. L. Cocke, C. D. Lin, M. Stockli, B. Walch, Y. D. Wang, R. E. Olson, V. D. Rodríguez, W. Wu, M. Pieksma, and N. Watanabe, Phys. Rev. A **54**, 1394 (1996).
[29] M. Abdallah, S. Kravis, C. L. Cocke, Y. Wang, V. D. Rodriguez, and M. Stöckli, Phys. Rev. A **56**, 2000 (1997).
[30] V. D. Irby, S. Datz, P. F. Dittner, N. L. Jones, H. F. Krause, and C. R. Vane, Phys. Rev. A **47**, 2957 (1993).
[31] R. D. DuBois, Phys. Rev. A **50**, 364 (1994).
[32] S. Ovchinnikov, G. Ogurtsov, J. Macek, and Y. Gordeev, Phys. Rep. **389**, 119 (2004).
[33] E. Y. Sidky, C. Illescas, and C. D. Lin, Phys. Rev. Lett. **85**, 1634 (2000).
[34] B. S. Nesbitt, M. B. Shah, S. F. C. O'Rourke, C. McGrath, J. Geddes, and D. S. F. Crothers, J. Phys. B **33**, 637 (2000).
[35] L. P. H. Schmidt, M. S. Schöffler, K. E. Stiebing, H. Schmidt-Böcking, R. Dörner, F. Afaneh, and T. Weber, Phys. Rev. A **76**, 012703 (2007).
[36] L. P. H. Schmidt, M. S. Schöffler, T. Jahnke, H. Schmidt-Böcking, and R. Dörner, Phys. Rev. A **109**, 032811 (2024).
[37] M. Pieksma, S. Y. Ovchinnikov, J. van Eck, W. B. Westerveld, and A. Niehaus, Phys. Rev. Lett. **73**, 46 (1994).
[38] G. Bandarage and R. Parson, Phys. Rev. A **41**, 5878 (1990).
[39] M. Pieksma and S. Y. Ovchinnikov, J. Phys. B **24**, 2699 (1991).
[40] M. Pieksma and S. Y. Ovchinnikov, J. Phys. B **27**, 4573 (1994).
[41] R. Dörner, H. Khemliche, M. H. Prior, C. L. Cocke, J. A. Gary, R. E. Olson, V. Mergel, J. Ullrich, and H. Schmidt-Böcking, Phys. Rev. Lett. **77**, 4520 (1996).
[42] C. Illescas, I. Rabadán, and A. Riera, Phys. Rev. A **57**, 1809 (1998).
[43] D. R. Schultz, C. O. Reinhold, P. S. Krstić, and M. R. Strayer, Phys. Rev. A **65**, 052722 (2002).
[44] I. B. Abdurakhmanov, A. S. Kadyrov, and I. Bray, Phys. Rev. A **94**, 022703 (2016).
[45] I. B. Abdurakhmanov, J. J. Bailey, A. S. Kadyrov, and I. Bray, Phys. Rev. A **97**, 032707 (2018).
[46] C. T. Plowman, K. H. Spicer, I. B. Abdurakhmanov, A. S. Kadyrov, and I. Bray, Phys. Rev. A **102**, 052810 (2020).
[47] K. H. Spicer, C. T. Plowman, I. B. Abdurakhmanov, S. U. Alladustov, I. Bray, and A. S. Kadyrov, Phys. Rev. A **104**, 052815 (2021).
[48] K. H. Spicer, C. T. Plowman, S. U. Alladustov, I. B. Abdurakhmanov, I. Bray, and A. S. Kadyrov, Eur. Phys. J. D **77**, 131 (2023).
[49] K. H. Spicer, C. T. Plowman, M. Schulz, and A. S. Kadyrov, Phys. Rev. A **108**, 022803 (2023).
[50] C. T. Plowman, I. B. Abdurakhmanov, I. Bray, and A. S. Kadyrov, Phys. Rev. A **107**, 032824 (2023).
[51] C. T. Plowman, K. H. Spicer, and A. S. Kadyrov, Atoms **11**, 112 (2023).
[52] C. T. Plowman, K. H. Spicer, M. Schulz, and A. S. Kadyrov, Phys. Rev. A **108**, 052809 (2023).
[53] S. U. Alladustov, C. T. Plowman, I. B. Abdurakhmanov, I. Bray, and A. S. Kadyrov, Phys. Rev. A **106**, 062819 (2022).
[54] S. U. Alladustov, C. T. Plowman, M. S. Schöffler, I. Bray, and A. S. Kadyrov, Phys. Rev. A **109**, 022805 (2024).
[55] S. U. Alladustov, I. B. Abdurakhmanov, A. S. Kadyrov, I. Bray, and K. Bartschat, Phys. Rev. A **99**, 052706 (2019).
[56] I. B. Abdurakhmanov, A. S. Kadyrov, I. Bray, and K. Bartschat, Phys. Rev. A **96**, 022702 (2017).
[57] I. B. Abdurakhmanov, A. S. Kadyrov, S. U. Alladustov, I. Bray, and K. Bartschat, Phys. Rev. A **100**, 062708 (2019).
[58] H. Gassert, O. Chuluunbaatar, M. Waitz, F. Trinter, H.-K. Kim, T. Bauer, A. Laucke, C. Müller, J. Voigtsberger, M. Weller, J. Rist, M. Pitzer, S. Zeller, T. Jahnke, L. P. H. Schmidt, J. B. Williams, S. A. Zaytsev, A. A. Bulychev, K. A. Kouzakov, H. Schmidt-Böcking *et al.*, Phys. Rev. Lett. **116**, 073201 (2016).
[59] O. Chuluunbaatar, K. A. Kouzakov, S. A. Zaytsev, A. S. Zaytsev, V. L. Shablov, Y. V. Popov, H. Gassert, M. Waitz, H.-K. Kim, T. Bauer, A. Laucke, C. Müller, J. Voigtsberger, M. Weller, J. Rist, K. Pahl, M. Honig, M. Pitzer, S. Zeller, T. Jahnke *et al.*, Phys. Rev. A **99**, 062711 (2019).
[60] I. B. Abdurakhmanov, I. Bray, D. V. Fursa, A. S. Kadyrov, and A. T. Stelbovics, Phys. Rev. A **86**, 034701 (2012).
[61] M. Schulz, R. Moshammer, D. Fischer, H. Kollmus, D. H. Madison, S. Jones, and J. Ullrich, Nature (London) **422**, 48 (2003).